Electronic Supplementary Material (ESI) for Lab on a Chip.
This journal is © The Royal Society of Chemistry 2023

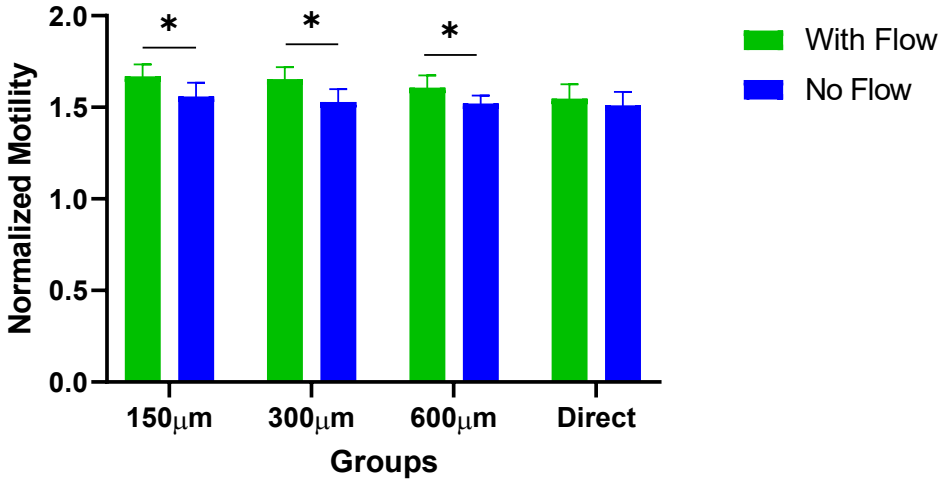

Fig. S1 Normalized motility of sperms obtained from microchannels with varying radii of curvature, as well as from a direct channel when there is (green) and there is not (blue) a gentle backflow (n=6, time=20 min). The motility values were normalized with the motility of the raw semen sample used in each with-flow and no-flow experiment to account for the use of two different semen samples. For channels with a curvature in their design, the presence of a backflow has significantly improved the motility of the selected sperms, compared to the no-flow condition, while in the case of a direct channel, no significant difference was observed between the no-flow and with-flow conditions. Moreover, when there is no backflow (blue bars), there is no significant difference between different channel designs regarding the motility of the selected sperm, which further confirms the crucial role of the backflow in the selection mechanism. These results highlight how the interplay of the BDR mechanism and backflow realizes highly-motile sperm selection. Different groups are compared using two-way ANOVA and Tukey test.

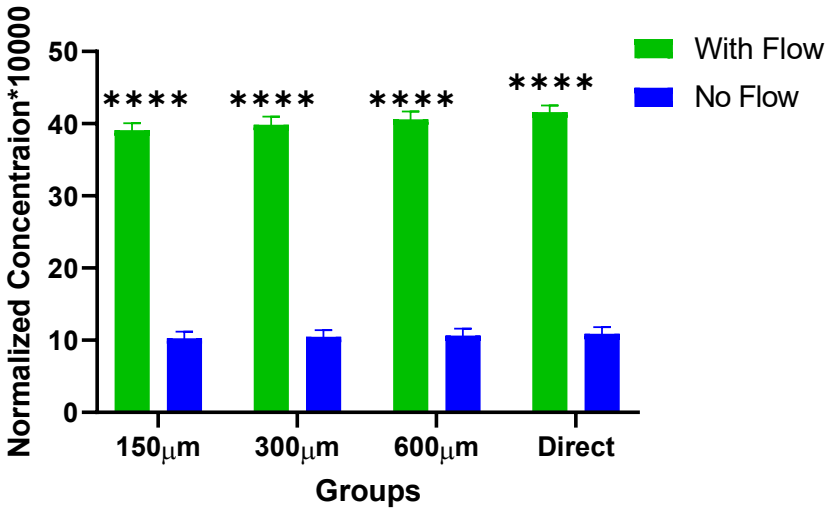

Fig. S2 Normalized concentration of sperms obtained from single microchannels with varying radii of curvature, as well as from a direct channel when there is (green) and there is not (blue) a gentle backflow (n=6, time=20 min). The concentration values were normalized with the concentration of the raw semen sample used in each with-flow and no-flow experiment to account for the use of two different semen samples. For all channels, the presence of a backflow has significantly improved the concentration of the selected sperms due to sperm rheotaxis. Different groups are compared using two-way ANOVA and Tukey test.

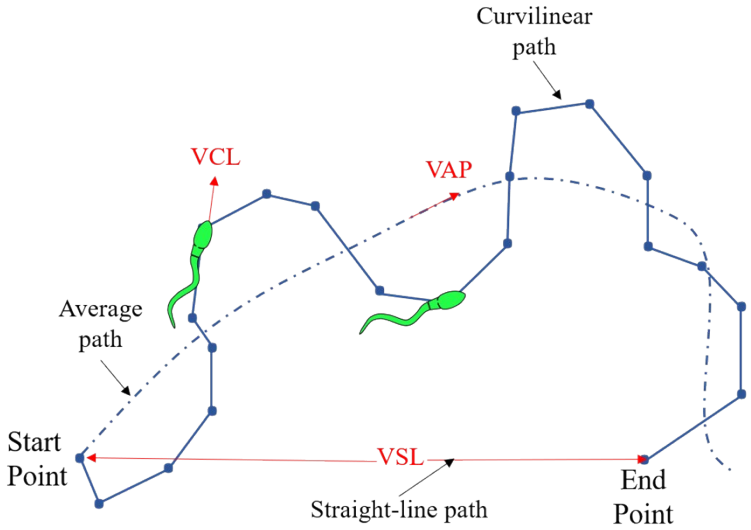

Fig. S3 Schematic of sperm movement and its corresponding velocities, namely, curvilinear velocity (VCL), straight-line velocity (VSL), and average-path velocity (VAP).

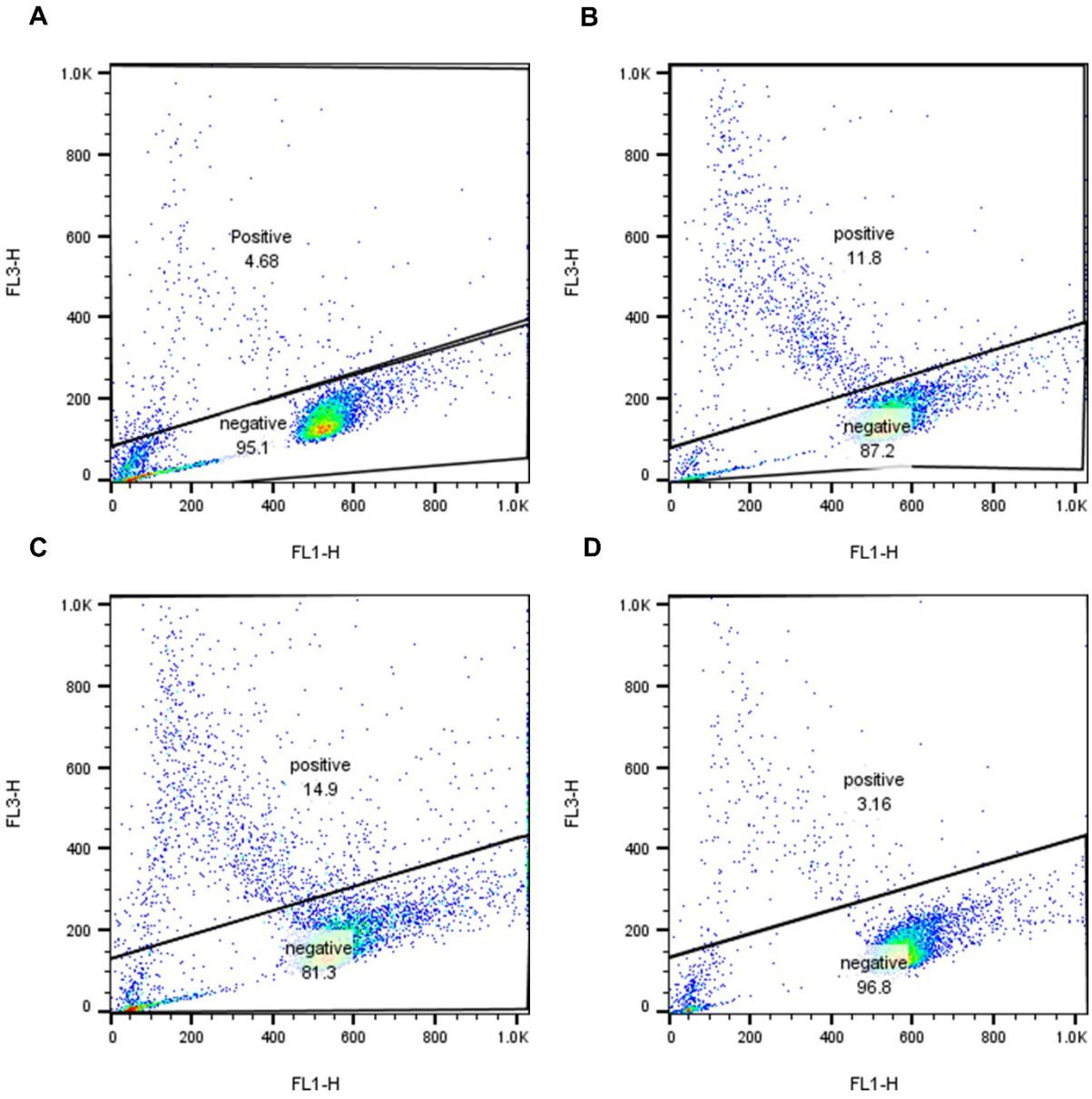

Fig. S4 Sperm chromatin structure assays (SCSAs) representation in dot plots dividing the selected sperms into two negative and positive populations – with positive regarded as having DFI – by (A) The chip, (B) DGC, (C) Raw semen and, (D) Swim up.

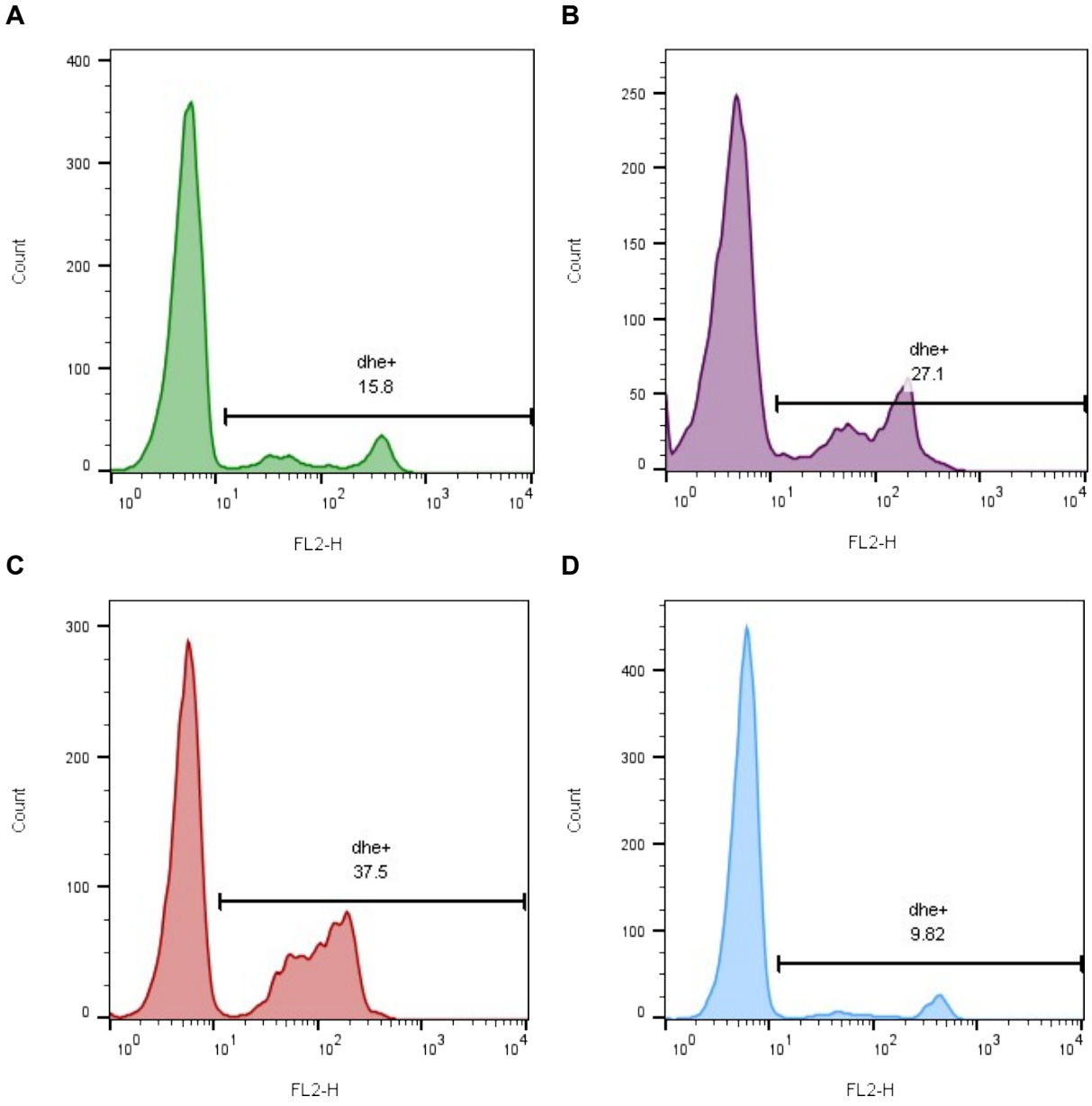

Fig. S5 The histogram chart of O^-_2 for the human sperms stained with DHE. (A)The chip, (B) DGC, (C) Raw semen, and (D) Swim up.

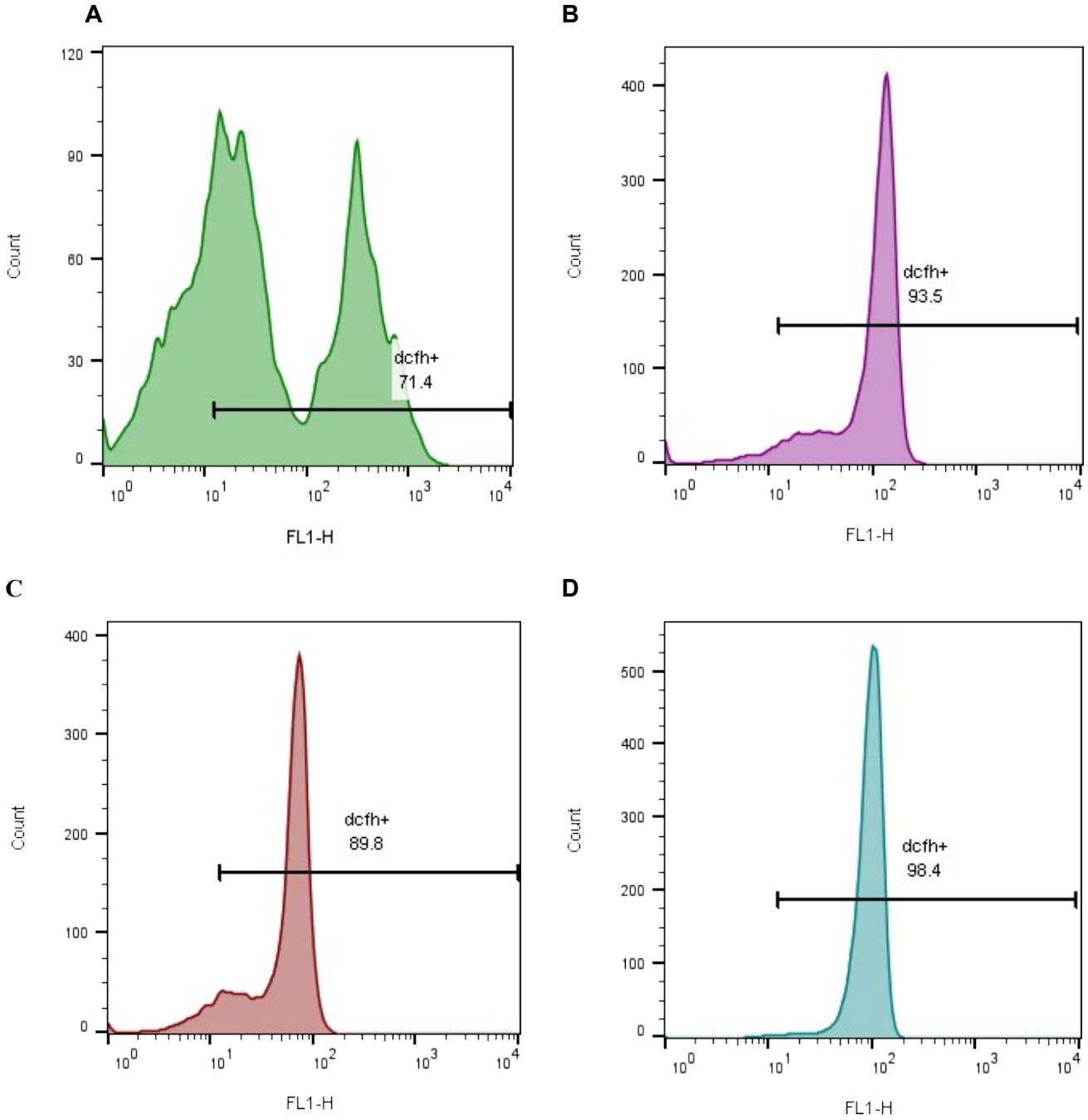

Fig. S6 The histogram chart of H_2O_2 for the human sperms stained with DHE. (A)The chip, (B) DGC, (C) Raw semen, and (D) Swim up.

Table S1: Motility, Viability, Kinematic Characteristic results (n=6), (Mean± Std. Deviation)

Parameters (n=6)	Groups				
	Raw	150 µm (single)	300 µm (single)	600 µm (single)	Direct (single)
% Total motility	56.69±0.7	94.53±1.27	93.99±1.35	91.08±0.88	87.68±1.58
% Progressive motility	35.96±1.56	88.49±2.92	85.90±3.30	82.12±1.65	77.95±2.53
Viability	63.10±1.56	95.66±0.95	95.00±1.34	92.33±0.95	91.33±1.60
VCL (µm/sec)	39.22±2.44	68.40±1.93	65.21±1.27	60.70±1.70	55.24±2.08
VSL (µm/sec)	20.92±1.35	61.30±1.43	57.50±1.37	50.41±1.69	42.39±1.62
VAP (µm/sec)	26.67±1.87	65.10±1.52	61.60±1.27	54.21±1.72	47.90±2.09
LIN	0.53±0.008	0.89±0.01	0.89±0.01	0. 83±0.008	0.77±0.004

Table S2: Motility, DFI, ROS, Kinematic Characteristic results (n=6), (Mean± Std. Deviation)

Parameters (n=6)	Groups			
	Raw	150 µm (parallel device)	Swim up	DGC
% Total motility	67.33±4.46	87.88±3.29	78.36±4.96	62.78±4.92
% Progressive motility	41.16±4.79	74.71±5.66	59.26±7.58	40.52±4.79
%DFI	16.35±3.3	6.12±0.93	4.73±0.25	20.67±3.6
VCL (µm/sec)	38.42 ± 1.98	68.43 ± 2.33	67.33 ± 4.9	55.19 ± 3.55
VSL (µm/sec)	20.98±1.62	49.75±0.83	29.30±2.93	27.78±2.86
VAP (µm/sec)	28.70±1.89	57.04±2.14	38.51±2.97	32.77±2.74
% ROS(H_2O_2)	85.30±3.41	76.48±3.28	94.12±3.27	91.53±3.06
%ROS(O_2^-)	24.66±5.27	14.83±2.15	12.82±1.62	27.17±6.20